Journal Pre-proof

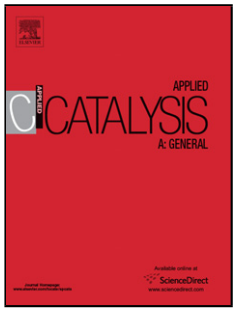

Na-Ce-modified-SBA-15 as an effective and reusable bimetallic mesoporous catalyst for the sustainable production of biodiesel

Edgar M. Sánchez Faba (Conceptualization) (Formal analysis) (Investigation) (Methodology) (Visualization) (Writing - original draft), Gabriel O. Ferrero (Conceptualization) (Funding acquisition) (Methodology) (Project administration) (Resources) (Supervision) (Writing - review and editing), Joana M. Dias (Conceptualization) (Methodology) (Writing - review and editing), Griselda A. Eimer (Conceptualization) (Funding acquisition) (Methodology) (Project administration) (Resources) (Writing - review and editing)

PII: S0926-860X(20)30362-8

DOI: https://doi.org/10.1016/j.apcata.2020.117769

Reference: APCATA 117769

To appear in: *Applied Catalysis A, General*

Received Date: 4 June 2020

Revised Date: 29 July 2020

Accepted Date: 1 August 2020

Please cite this article as: Faba EMS, Ferrero GO, Dias JM, Eimer GA, Na-Ce-modified-SBA-15 as an effective and reusable bimetallic mesoporous catalyst for the sustainable production of biodiesel, *Applied Catalysis A, General* (2020), doi: https://doi.org/10.1016/j.apcata.2020.117769

Na-Ce-modified-SBA-15 as an effective and reusable bimetallic mesoporous catalyst for the sustainable production of biodiesel

Edgar M. Sánchez Faba[a], Gabriel O. Ferrero[a‡], Joana M. Dias[b], Griselda A. Eimer[a*]

[a]CITeQ-CONICET-UTN, Universidad Tecnológica Nacional, Facultad Regional Córdoba, Maestro López esq. Cruz Roja, Ciudad Universitaria, CP: X5016ZAA, Córdoba, Argentina. Tel.: +54 0351 4690585; fax: +54 0351 4690585.

[b]Departamento de Engenharia Metalúrgica e de Materiais, LEPABE, Faculdade de Engenharia, Universidade do Porto, R. Dr. Roberto Frias, 4200-465 Porto, Portugal.

* Corresponding author e-mail address: geimer@frc.utn.edu.ar

‡ Co-corresponding author e-mail address: gferrero@frc.utn.edu.ar

Graphical abstract

Highlights

- 5 wt% of Na and 20 wt% of Ce led a material with good structure and basicity.
- FAME contents within EN 14214 limits were obtained using 5Na/20Ce/SBA-15 catalyst.
- 5Na/20Ce/SBA-15 was used 5 consecutive times without significant loss of activity.
- Ce addition contributes to catalyst stability protecting active species.

- Produced biodiesel meets key quality properties established by EN 14214.

Abstract

With the purpose to compete with the homogeneous catalytic biodiesel production, a highly efficient bimetallic solid catalyst with high exposed surface, high basicity, and reusable throughout several reaction cycles, was developed by doping SBA-15 with sodium and cerium in different concentrations. The catalyst with 5 wt% of sodium and 20 wt% of cerium showed good structural ordering and had the highest basicity due to the presence of a large amount of medium and strong sites compared to the other materials. It was effectively used as a solid base catalyst for biodiesel production from sunflower oil and absolute methanol. The highest FAME content (98.9 wt%) was achieved under optimum conditions of 40:1 methanol/oil molar ratio, 10 wt% catalyst loading, 60 °C, stirring speed of 600-700 rpm and 180 min. Further, this material was reused for five consecutive runs, obtaining FAME contents greater than 90% in each one of them.

Keywords: BIODIESEL, SODIUM; CERIUM; MESOPOROUS MATERIALS; REUSABLE; TRANSESTERIFICATION

---

1. Introduction

Fatty acid alkyl ester (FAAE), better known as biodiesel, is a substitute for petroleum diesel fuel. It can be used directly on diesel engines because of their similar properties, or in proper blends [1].

Due to conventional fossil fuel depletion given by the growth of population, transportation, and industrialization, biodiesel has attracted more attention since it can be obtained from renewable raw materials such as vegetable oils (edible and non-edible) and animal fats [2,3]. Further, it has many advantages over fossil energy sources: high flashpoint, higher combustion efficiency, higher

cetane number, better lubrication, noncorrosive, a positive impact on the fossil fuel footprint, environmental compatibility owing to its lower emissions, biodegradability, renewability, and negligible toxicity [1,2,4–6].

Biodiesel is generally produced by a transesterification reaction or alcoholysis. The main objective of this process is to reduce the viscosity and density of the starting oil/fat and improve the properties of the fuel by producing alkyl esters when triglycerides react with a short-chain alcohol [7,8]. When methanol is employed as alcohol, fatty acid methyl esters are generated, usually known by its acronym FAME. In all cases, glycerol is generated as a byproduct [9,10].

The possibility of reducing the environmental impact that the homogeneous industrial process generates has made the research focus not only on the need to maximize conversions and yields but also on the development of benign and non-corrosive solid catalysts that can be reused and minimize the requirement of final product purification stages for its commercialization [6,10–12]. With this purpose, materials with both acid and basic properties, as well as biocatalysts which incorporate enzymes, have been synthesized, characterized, and tested in the transesterification of different substrates [13–18]. Catalysts with basic properties are preferred since the reaction rate is considerably higher than that catalyzed by an acid, and it uses mild reaction conditions [9,19].

On the other hand and as it is already known, the transesterification of vegetable oils and fats with a short-chain alcohol is a reversible process. According to the reaction stoichiometry, three moles of alcohol are required per mole of triglyceride to obtain three moles of alkyl esters of fatty acids and one of glycerol [20]. However, to achieve high FAME yields, alcohol is frequently added in excesses (in different molar ratios respect to the oil loading) to shift the balance in the desired product direction [21]. Moreover, when working with heterogeneous catalysis and given the existence of three different phases (alcohol + oil + solid catalyst), the reaction rates are usually lower than those of the homogeneous processes. Therefore, longer times are required to reach the equilibrium state. This can also be improved by increasing the alcohol content in the reaction

mixture, as well as by modifying the temperature, mixing rate, reactants purity, catalyst type and charge [8,22].

Within the variety of solid basic catalysts that are currently produced, those supported on mesoporous silica are of interest since the dispersion of the active phase on a large specific surface (>800 m^2) usually generates a better active site availability and promotes mass transfer [23,24]. However, one of the drawbacks of using these materials is the leaching of the active species to the reaction mixture, which considerably reduces the useful life of the catalyst [25–28].

In a previous research, it was demonstrated that supporting sodium on mesoporous SBA-15 results effective for the transesterification of sunflower, soybean and frying oil with absolute methanol. At 5 h and 60 °C, FAME contents greater than 96 wt% were obtained with a catalyst charge of 8 wt% and a 14:1 methanol to oil molar ratio. Nevertheless, the FAME content dropped to 83 wt% in the second reaction cycle due to the partial leaching of sodium species [16].

Several alternatives to mitigate this disadvantage are being studied. Among them, the development of bimetallic materials, thereby stabilizing the active phase by adding another metal to the support can be considered. Additionally, this second metal could act in synergism with the former and confer to the catalyst new properties which favor the reaction [29].

In the case of biodiesel production, it has been reported the effect of combining alkali and alkaline earth metals with other metals, such as cerium (Ce), zirconium (Zr) and zinc (Zn), either by direct synthesis or by impregnation, to obtain bimetallic catalysts. This would help to increase the activity promoting a higher basic strength, and to improve the stability of the material, making possible to reuse it over several reaction cycles without further loss of the active species [6,30].

Chen et al. used a Na/Zr-SBA-15 catalyst, obtaining FAME yields between 85-88% by reacting rapeseed oil with methanol (70 °C, 6 h, 12 wt% of catalyst and 6:1 methanol/oil molar ratio). Nonetheless, after the first cycle, the activity fell around 12-15%, remaining constant in the two subsequent cycles [31]. Thitsartarn et al. incorporated cerium into the SBA-15 structure during the synthesis and then impregnated calcium in different concentrations. The material with a Si/Ce molar ratio of 5 and 30 wt% of Ca showed the highest activity in the production of FAME from

palm oil and methanol, with a yield of 87% in 6 h (5% of catalyst, 85 °C, 20:1 methanol/oil molar ratio). This catalyst was used in several consecutive cycles with the yield being reduced up to 75% [27]. Malhotra et al. synthesized materials based on SBA-15 doped with lithium and cerium. Despite obtaining solids with a low specific area (~148-103 m^2/g), possibly due to the structural deterioration generated by lithium on the mesoporous silica, the catalyst gave biodiesel yields over 95% and was successfully used for 5 cycles after optimizing reaction conditions [21].

In terms of homogeneous catalytic systems, sodium is one of the most employed alkaline metals (normally as hydroxide) owing to its relatively low price and high basic strength, which provides high reaction rates [8]. However, regarding heterogeneous catalytic systems, even though sodium-modified-materials result in highly basic properties and high catalytic activity in transesterification, they do not usually maintain good stability and, therefore, good yields over several reaction runs, as previously mentioned.

The present work exposes the use of cerium to enhance the reusability capacity of catalysts constituted by sodium supported on SBA-15. We focus on a possible shielding effect of cerium on sodium-doped-mesoporous material to enhance its stability, which has not been studied in detail in the literature until date.

The synthesized materials were employed in the transesterification of sunflower oil with absolute methanol to produce biodiesel. A study of the impact of alcohol to oil molar ratio and catalyst charge was made to obtain FAME contents that meet the international standards. Further, the reusability of the best catalyst was evaluated under optimized reaction conditions to verify its stability through several reaction runs.

Finally, achieving the FAME content established by the norms is not enough for the biofuel to be marketable. Many investigations ignore this point and therefore more studies in this regard are necessary. This is why, in addition to purity, density, kinematic viscosity, acid value and moisture content of the biodiesel produced by this route were tested to verify that they complied with international standards for its commercialization and use for transportation and industry purposes [32].

---

2. Experimental

2.1. Synthesis and characterization of the catalysts

SBA-15 was synthesized by the hydrothermal process [33–35]. Triblock copolymer Pluronic 123 (Aldrich) was used as a structure-directing agent and tetraethyl orthosilicate (TEOS, Aldrich) as the silicon source; meanwhile, a solution of hydrochloric acid (HCl, Cicarelli) was employed to regulate the pH. Reagents were stirred at 40 °C for 20 h and then aged into a Teflon autoclave, under static conditions at 80 °C for 24 h. The obtained suspension was filtered, washed with distilled water and dried at 60 °C overnight. The recovered powder was finally calcined at 500 °C for 8 h, using a heating rate of 1 °C/min [36].

The mesoporous support was doped by the wet impregnation method. Sodium and cerium nitrates ($NaNO_3$, Mallinckrodt and $Ce(NO_3)_3{\cdot}6H_2O$, Aldrich) were used as metal sources. The theoretical sodium loadings were 5 and 10 wt%, related to the final catalyst mass. The cerium loading was maintained at 20 wt%, since it was reported to be the optimum to give good stability to the catalyst [21]. Firstly, the salts were dissolved in distilled water and then, the support was added (0.08 g/mL of solution). The suspension was stirred at ambient temperature for 6 h. After this, the solvent was evaporated in an oven at 100 °C overnight. Finally, the materials were calcined at 550 °C for 5 h, using an 8 °C/min heating rate, which is the known to promote a good dispersion of the active phase on the support [36]. The obtained catalysts were named XNa/YCe/SBA-15, where X and Y represent the theoretical metal loadings in weight percentage.

Small-angle X-ray scattering (SAXS) analysis was performed using a Xenocs XEUSS 2.0 equipment provided with a Pilatus 100 K detector and CuKα radiation (λ=0.154 nm). Measures were made in the 2θ range of 0.3-11°. High-angle X-ray diffraction (XRD) patterns were recorded on a

PANalytical X-Pert Pro X-ray powder diffractometer, with a Bragg-Brentano geometry. A CuKα lamp was employed (40 kV, 40 mA), in a 2θ range between 20-80°.

High-resolution transmission electron microscopy (HR-TEM) images were taken on a JEOL JEM-2100 Plus microscope with an acceleration voltage of 200 kV, and equipped with an Oxford X-MAX 65 T energy dispersive spectrometer (EDS).

The specific surface of the materials was measured by the Brunauer–Emmett–Teller (BET) method, employing a Micrometrics Pulse ChemiSorb 2700 equipment.

Carbon dioxide temperature-programmed desorption (CO_2 TPD) profiles were recorded on a Micromeritics ChemiSorb 2720 equipment. Samples were treated at 150 °C for 30 min under nitrogen flow (20 mL/min). Then, the temperature was set at 80 °C, and CO_2 (50 mL/min) was introduced for one hour. Once the excess of CO_2 was purged with He (20 mL/min for 45 min at 100 °C), samples were heated up to 950 °C using a ramp of 10 °C/min. A conductivity detector was used to measure the desorbed CO_2.

X-ray photoelectron spectroscopy (XPS) analysis was performed on a Thermo Fisher Scientific K-Alpha$^+$ X-ray Photoelectron Spectrometer, equipped with an Al X-ray source. Data was analyzed by employing the software Thermo Avantage 5.9912.

2.2. Catalytic activity

Reactions were carried out for 5 h in a three-neck flat-bottom flask placed on a hot plate with a magnetic stirrer and connected to a reflux condenser. Sunflower oil (Cocinero) and absolute methanol (Sintorgan) were used as reagents. The initial catalyst loading was 8 wt% referred to the oil mass [16]; meanwhile, alcohol to oil molar ratio was varied between 14:1 and 40:1. The temperature was maintained at 60 °C and magnetic stirring at 600-700 rpm. During the run, samples were taken at different times.

After 5 h, the catalyst was recovered by filtration and the excess of methanol was recovered in a rotary evaporator. To ensure the separation of biodiesel and glycerol, products were settled in a separatory funnel overnight. Finally, biodiesel was kept in a freezer (-18 °C) until its analysis. Before the next reaction cycle, the catalyst was washed with acetone (~5 mL) and calcined for 5 h at 550 °C with a heating rate of 8 °C/min.

All reactions were performed at least in duplicate. The results are expressed as mean values, with relative percentage differences between them always less than 5% of the mean.

2.3. Biodiesel quantification and characterization

Reaction products were quantified by Fourier Transform Infrared Spectroscopy (FT-IR) following the method described by Mahamuni et al. [37]. A Thermo Scientific Nicolet iS10 Spectrometer equipped with a horizontal attenuated total reflectance (ATR) accessory was employed. Each spectrum was taken in the range between 650-4000 cm^{-1}, with a 4 cm^{-1} resolution and 50 scans per sample. The fatty acid methyl esters were quantified measuring the height of the bands at 1436 and 1196 cm^{-1} (CH_3 asymmetric bending and O–CH_3 stretching vibration of methyl esters, respectively) respect to a baseline located parallel to the abscissa axis and that intercepted the spectra at a wave number of 2000 cm^{-1} (one base). Lipids were quantified in the same way employing the bands at 1097 and 1377 cm^{-1} (O–CH_2–C asymmetric axial stretching of triglycerides and O–CH_2 groups in glycerol moiety of mono, di, and triglycerides, respectively. See Fig. S1 in *Supplementary Material*). For calibration, patterns were prepared by mixing B100 with sunflower oil in different mass percentages (10–90 wt %), and Thermo Scientific™TQ Analyst™9.7 Software was employed to construct the calibration curves (band height vs. FAME wt% and band height vs. lipids wt%). The technique was validated by high performance liquid chromatography, using a Perkin Elmer Series 200 HPLC was used, equipped with a UV/visible detector, a Vertex Plus (250 mm x 4.6 mm, 5µm) Eurospher II 100-5 C18P column. In this way, it is possible to

quantify FAME with an accuracy that varies between 97.4-99.9% for concentrations above 20% by weight.

Biodiesel acid value was determined by volumetric titration according to the standard EN 14104 (2003). An aqueous solution of KOH 0.1 M was used as a titrant, 2-propyl alcohol as a solvent, and an ethanolic solution of phenolphthalein as the end point indicator. Results are expressed in mg of KOH per g of sample.

Water content was measured using the Karl Fischer titration technique, following the standard EN ISO 12937 (2003). A Metrohm 899 Coulometer (Herisau, Switzerland) was used.

The kinematic viscosity was measured at 40 °C, according to the standard ASTMD 445-06. An IVA Cannon-Fenske glass routine viscometer series 100 (Buenos Aires, Argentina) was employed.

---

3. Results and discussion

3.1. Catalysts characterization

Small-angle X-ray scattering was employed to corroborate the pore ordering of the synthesized support and its permanence after doping it with the different metal loadings. The resulting SAXS patterns are shown in Fig. 1. The SBA-15 exhibits three well-resolved peaks, indexed to the diffraction of planes (1 0 0), (1 1 0) and (2 0 0), typical of a 2D hexagonal pore arrangement (*p6mm*) [33,34]. After cerium and sodium impregnation, the periodic-ordered structure of SBA-15 remains for the 20Ce/SBA-15 and 5Na/20Ce/SBA-15 catalysts; however, the intensity of the peaks decreases possibly because of the decreasing scatter contrast between pore walls and space with the introduction of metal species [26]. This can also be observed in the decrease of the specific surface of the materials as the metal loading increases (see Table 1). 10Na/20Ce/SBA-15 only shows the peak corresponding to the plane (1 0 0) with low intensity, which indicates a loss of the support ordered structure in agreement with its low exposed area (95 m^2/g). According to

Thitsartarn et al., the process of calcination at high temperatures could reduce the leaching of active species by enhancing their interaction with the support; nonetheless, the material could inevitably lose some of specific surface and basicity by sintering process [6]. Here, although all synthesized catalysts were submitted to calcination, its effect was more marked for 10Na/20Ce/SBA-15, probably due to the increased presence of Na species, such as sodium oxides, that can partially block some mesopores and favor the collapse of the structure during the high-temperature treatment [36,38,39]. This behavior was reported by Chen et al. when Na was incorporated into Zr-SBA-15 catalysts by wet impregnation [31].

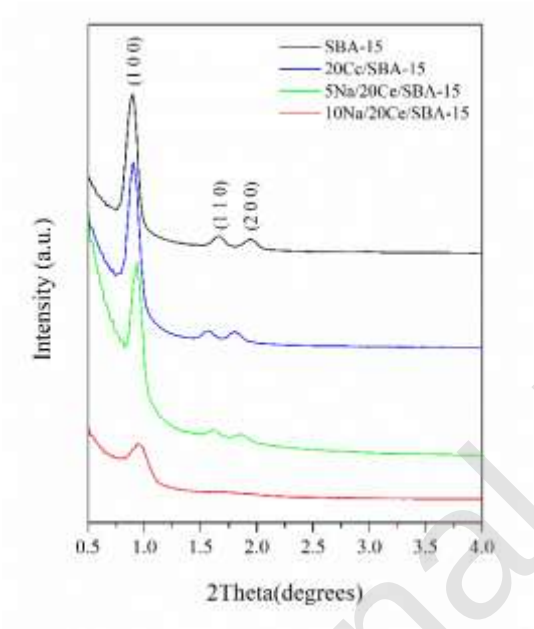

Fig. 1. SAXS patterns of the synthesized materials.

Table 1. Specific surfaces of the synthesized materials.

Material	Specific surface (m^2/g)
SBA-15	811
20Ce/SBA-15	439
5Na/20Ce/SBA-15	263
10Na/20Ce/SBA-15	95

High-angle XRD patterns of the metal-modified materials (Fig. 2) present the characteristic peaks of a fluorite-type cubic structure *Fm3m* (JCPDS no. 034-0394) of cerium oxide (CeO_2) [21,40]. This phase may be segregated on the support surface. On the other hand, no peaks corresponding to sodium species are observed, evidencing that they could be finely dispersed on the silica support [36]. As expected, SBA-15 only shows the amorphous-silica peak at 2θ = ~22° [41].

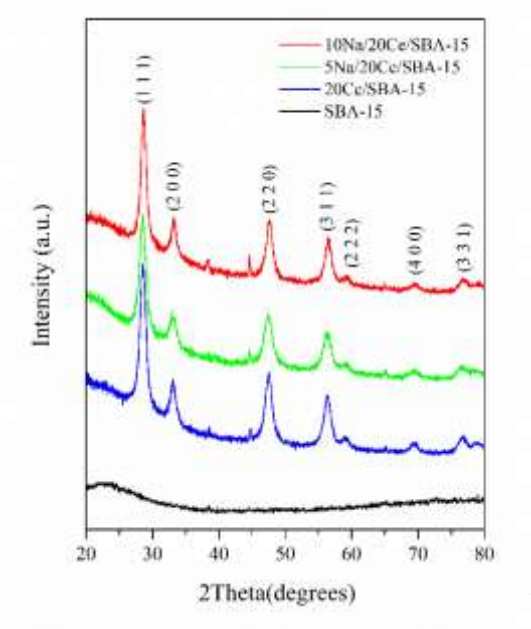

Fig. 2. High-angle XRD patterns of the synthesized materials.

TEM images were used to study the nanostructure of the materials. As can be seen in Fig. 3 a-b, the SBA-15 shows the typical hexagonal and parallel pore arrangement in agreement with the SAXS and XRD patterns. The pore diameter estimated from the images is ~5 nm while the wall thickness is about 4 nm. When Ce is incorporated (Fig. 3 c-d), ceria crystals covering the surface are observed, confirming the presence of crystalline phases as seen by XRD, although the long-range channel ordering of the mesoporous support remains. Then, the detriment of the 20Ce/SBA-15 specific area could be produced by a partial blocking of the mesopores owing to such CeO_2 phase, as already informed by Pal et al. [42]. 5Na/20Ce/SBA-15 (Fig. 3 e-f) also preserves the ordered channel structure of the support even though its area value is lower than

20Ce/SBA-15, possibly due to the combined effect of metal loadings; nevertheless, 10Na/20Ce/SBA-15 (Fig. 3 g-h) does not seem to maintain the original mesoporous structure because no channels can be seen. This confirms the conclusions drawn from the SAXS pattern and the specific surface value. In agreement, 5 wt% of Na is the most suitable loading to achieve a catalyst with good structure.

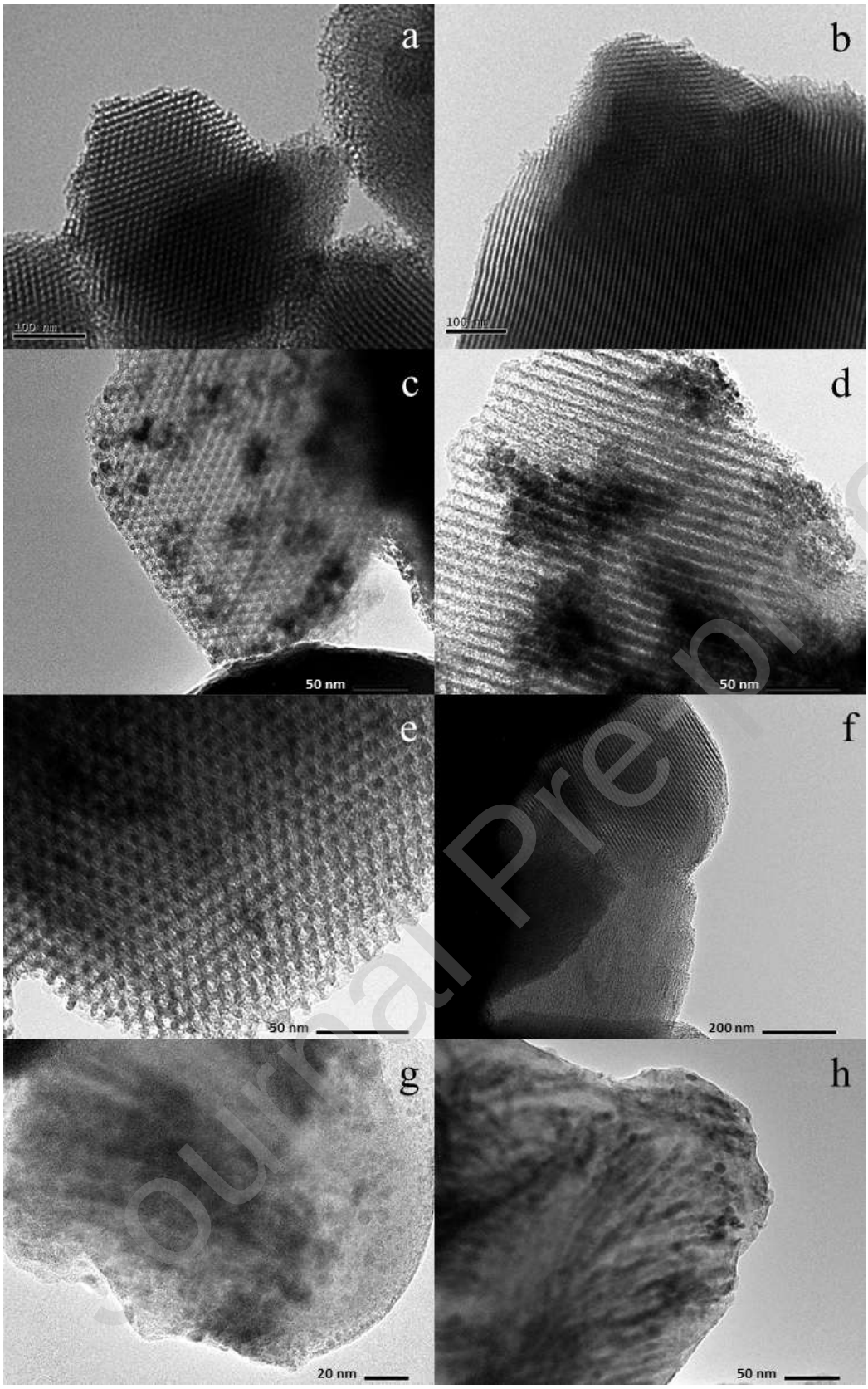

Fig. 3. TEM images of SBA-15 (a, b), 20Ce/SBA-15 (c, d), 5Na/20Ce/SBA-15 (e, f) and 10Na/20Ce/SBA-15 (g, h).

The elemental mapping of 5Na/20Ce/SBA-15 catalyst (Fig. 4) and the TEM-EDS spectrum (see Fig. S2 in *Supplementary Material*) ratify the loading and the good dispersion of cerium and sodium throughout the siliceous support surface; meanwhile, the distribution of the elements along 10 aligned points for the three metal-modified catalysts can be seen in the graphs of the EDS linear chemical composition analysis (see Fig. S3 in *Supplementary Material*).

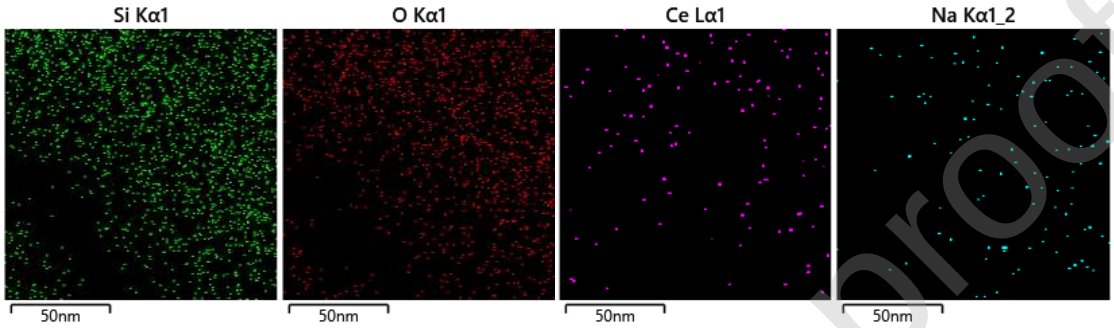

Fig. 4. Elemental mapping of 5Na/20Ce/SBA-15 catalyst.

The basicity and basic strength of the catalysts was studied by carbon dioxide temperature-programmed desorption. As explained by Wen et al., the complexity of the obtained profiles (Fig. 5) evidences the heterogeneity of the surfaces of the catalysts, since CO_2 interacts with oxygen atoms of different chemical nature, with different binding energy and coordination [43]. In this way, the strength of sites increases as the peaks move to high temperatures in the TPD profile, and the area under the curve is proportional to the number of sites.

The desorption band in the approximate range of 70-250 °C is attributed to weak basic sites, given by adsorption of the probe molecule on –OH species of the siliceous support [6,26]. As expected, SBA-15 only exhibits a peak in this region. The interval between 250-600 °C represents the adsorption of CO_2 on medium basic sites [26]. The 5Na/20Ce/SBA-15 catalyst stands out from the other materials in this region, evidencing the main presence of species such as sodium silicates as previously reported [36]. However, the 20Ce/SBA-15 also shows a weak band in this zone. Meanwhile, the region from 600 °C onwards is due to the existence of super basic species, such as

sodium oxides [26,39]. The 10Na/20Ce/SBA-15 exhibits a marked peak in this area, demonstrating its highest basic strength, which could also be responsible for its lack of structure: despite its thick pore walls, SBA-15 seems not to be resistant to high loadings of strong alkali metals as already reported [36,44].

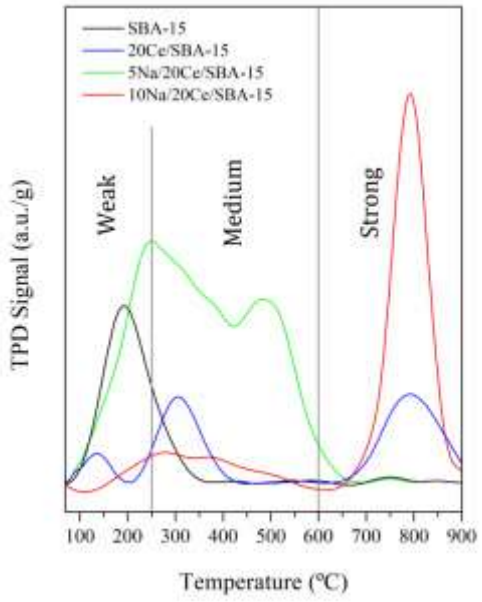

Fig. 5. CO_2 TPD profiles of the synthesized materials.

Table 2 shows the quantification of weak, medium and strong basic sites in the materials, measured as mmol of desorbed CO_2 per gram of sample. As can be seen, SBA-15 has a small number of basic sites, and they are mainly weak. The amount of medium and strong sites increases with the incorporation of the metals. Many authors describe that CeO_2-dopped-SBA-15 consists of both Lewis acid and basic sites due to the presence of exposed and highly mobile O^{2-} ions. Nevertheless, the basic strength of CeO_2 is less than that of alkali metals [21,42]. This fact together with the presence of ceria crystalline phases evidenced by XRD and TEM could explain why the amount of basic sites on the 20Ce/SBA-15 catalyst is small despite the high metal loading [30]. After a simultaneous co-impregnation procedure of SBA-15 with both metals (Na and Ce), the total basicity increases for 5Na/20Ce/SBA-15. This sample shows the highest presence of medium

basic sites, possibly caused by the preferred formation of silicate species rather than oxide species due to a better dispersion of sodium on silica [26]. Nevertheless, when Na content increases up to 10 wt%, the total basicity decreases, although 10Na/20Ce/SBA-15 shows the highest proportion of strong sites. This can be explained by the fact that the ordered structure of 10Na/20Ce/SBA-15 has collapsed, restricting the availability of sites despite the higher sodium content [6]. Ayoub et al. reported that high loadings of strong alkalis could react with the silica support and produce the collapse of the structure when those strongly basic species are formed during calcination [44].

Table 2. CO_2 adsorption capacity on the different catalysts.

Material	Basicity[a] ($mmolCO_2/g_{catalyst}$)			Total basicity ($mmolCO_2/g_{catalyst}$)
	Weak ~70–250 °C	Medium ~250-600 °C	Strong ~600–900 °C	
SBA-15	0.23	0.05	0.00	0.28
20Ce/SBA-15	0.02	0.12	0.17	0.31
5Na/20Ce/SBA-15	0.25	0.76	0.03	1.04
10Na/20Ce/SBA-15	0.01	0.07	0.47	0.55

[a] Calculated from the integrated areas of TPD bands.

XPS study was employed to determine the chemical environment and the electronic state of the different elements present on the catalysts, as well as the interactions of the doped-metals with the silica network. Fig. 6 shows the spectra regions of Si 2p, O 1s, Na 1s and Ce 3d for the synthesized materials, while Table 3 shows the binding energies corresponding to each peak. C 1s signal was corrected to 284.8 eV for all the samples.

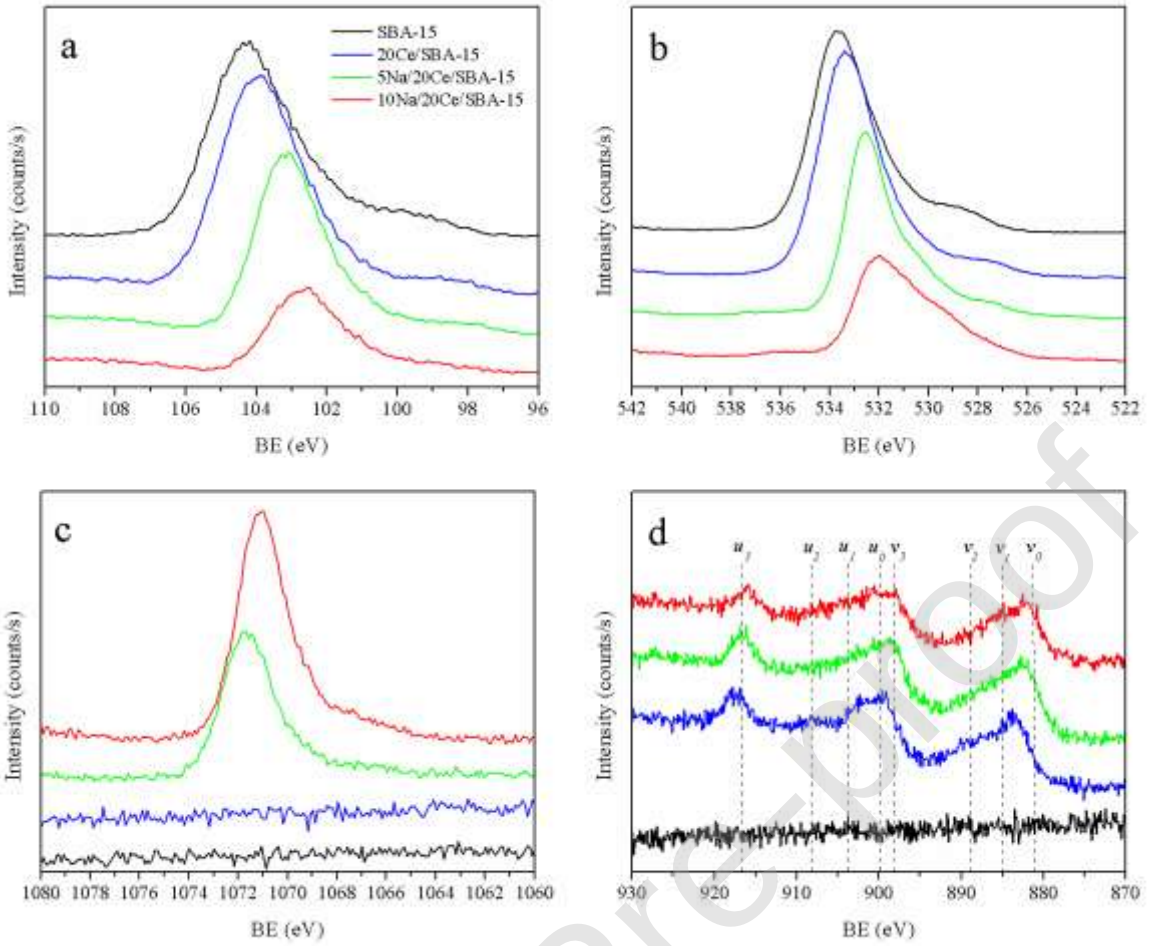

Fig. 6. XPS spectra of regions: (a) Si 2p, (b) O 1s, (c) Na 1s and (d) Ce 3d of the synthesized materials.

It should be mentioned that the observed shoulders at lower binding energy in addition to the main peak in the Si, O and Na regions may be owing to a difference in the charge compensation between the materials surface and the mesopores.

Si 2p spectra correspond to the presence of SiO_2 species of the siliceous support. According to Malhotra et al., this signal is due to the contribution of Si-O bonds and $SiOH_2^+$ species over the catalyst surface. The shift of this band to lower binding energies for the modified materials compared to the pure SBA-15 (from 104.3 to 102.8 eV), suggests the existence of a strong interaction between the impregnated metals and the support (see Fig. 6-a and Table 3) [21,36,45].

Table 3. Binding energy and assignment of Ce 3d XPS data for the synthesized materials.

Material	Si 2p (eV)	O 1s (eV)	Na 1s (eV)	Ce 3d[a] (eV)							
				Ce $3d_{5/2}$				Ce $3d_{3/2}$			
				v_0	v_1	v_2	v_3	u_0	u_1	u_2	u_3
SBA-15	104.3	533.6	-	-	-	-	-	-	-	-	-
20Ce/SBA-15	104.0	533.4	-	883.2	886.6	889.9	899.0	902.1	905.5	908.8	917.1
5Na/20Ce/SBA-15	103.2	532.6	1071.7	881.7	884.7	888.3	897.7	900.1	903.3	907.2	916.4
10Na/20Ce/SBA-15	102.8	532.1	1071.1	881.7	885.0	888.4	897.5	900.4	903.9	907.3	915.9

[a]Ce 3d assignment was made according to the deconvoluted spectra (see Fig. S4 in *Supplementary Material*).

The Ce 3d signal shows multiple peaks in the binding energy range of 875-925 eV. The spectra were deconvoluted into eight peaks corresponding to four doublets associated with $Ce3d_{5/2}$ (v) and $Ce3d_{3/2}$ (u) spin-orbit coupling states (see Fig. S4 in *Supplementary Material*). As described by Zhang et al., the doublets (v_0, u_0), (v_2, u_2) and (v_3, u_3) can be identified with the $3d^{10}$ $4f^0$ state of Ce^{4+}, while the doublet (v_1, u_1) is characteristic of the $3d^{10}$ $4f^1$ state of Ce^{3+} (see Table 3 and Fig. 6-d) [21,40,46]. Bêche et al. stated that the presence of the contribution in the range of 915-917 eV (u_3) for the three catalysts loaded with cerium, and associated with the $Ce3d_{3/2}$, is a fingerprint of tetravalent cerium (Ce^{4+}). Then, this signal confirms the existence of the ceria phase on the mesoporous support [47].

Na 1s symmetric signal appears for the metal loaded materials at ~1071 eV, confirming the incorporation of sodium on the support surface (see Fig. 6-c and Table 3) [36].

Finally, O 1s signal is mostly attributed to the oxygen atom present in the form of SiO_2 in the support. Meanwhile, many authors reported that lattice oxygen of ceria and sodium species also contribute for the metal-modified-materials, making the peak asymmetric as observed in Fig. 6-b. Thitsartarn et al. reported that the surface oxygen species and, therefore, the shifting of BE O 1s signal correlates to the basic strength of solid catalysts. This is why these species should be studied to understand the basic properties and catalytic behaviors of the synthesized materials. The transference of electrons to oxygen species of the catalysts (electron pair donation) leads to the electron-rich property of the surface oxygen species (electron acceptor), which increases the

basic strength of the active sites. This electron transfer is evidenced by the shift of the O 1s signal to lower binding energy values [27]. In this way, the slight shifting of O 1s signal to lower values compared to SBA-15 (from 533.6 to 533.4 eV), provides scarcely significant Lewis basicity to 20Ce/SBA-15 catalyst, as verified by CO_2-TPD [6,42]. When SBA-15 is impregnated with both metals (sodium and cerium), the shifting of the O 1s band becomes more marked, as observed in Fig. 6-b. This result is in good agreement with the literature, in which the reduction properties of cerium-doped with alkali was reported [6]. Consequently, it can be deduced that the greater shifting of O 1s signal in 5Na/20Ce/SBA-15 and 10Na/20Ce/SBA-15 catalysts to lower position as compared to the 20Ce/SBA-15 catalyst and the pure support (see Fig. 6-b and Table 3) is due to sodium species incorporation. This correlates to the higher basic strength of these materials and gives account for the presence of exposed and highly mobile O^{2-} ions on the catalyst surface, which is in agreement with CO_2-TPD analysis results [27].

3.2. Catalytic activity

The synthesized materials were tested on the transesterification of commercial sunflower oil with absolute methanol to produce FAME, according to the optimum reaction conditions previously established and published for Na/SBA-15 materials [16]. The results are displayed in Fig. 7.

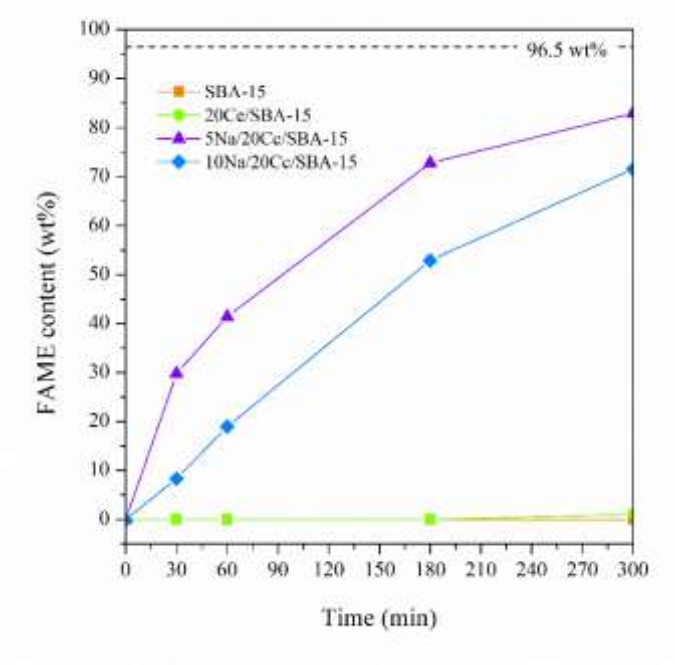

Fig. 7. FAME content vs. reaction time employing the synthesized catalysts. Reaction conditions: 8 wt% of catalyst, 14:1 alcohol to oil molar ratio, 60 °C, magnetic stirring at 600-700 rpm, and 5 h. The dashed line indicates the minimum limit according to European standard EN 14214.

As expected, the mesoporous support (SBA-15) produced negligible FAME owing to the lack of active sites for transesterification. As seen on CO_2-TPD patterns, SBA-15 only has a small quantity of weak basic sites due to its poor ability to adsorb CO_2, which does not catalyze the reaction [39]. When using 20Ce/SBA-15 as a catalyst, less than 2 wt% of FAME was obtained. This behavior can be explained taking into account that although this material has medium and strong basic sites (Table 2 and Fig. 5), its total basicity as well as the basic strength are still low, characteristic also confirmed by XPS. Additionally, the big ceria crystals observed by TEM have less exposed surface, and these crystalline phases may not favor the reaction as already informed [36].

Then, sodium loading is necessary to generate active sites that carry out the transesterification reaction [27]. As seen in CO_2-TPD patterns and XPS, sodium promotes the generation of medium and strong basic sites on the catalyst surface and essential for the reaction to take place [48]. As Ambat et al. reported, methanol is adsorbed on Lewis and Brønsted basic sites of the solid catalyst

and forms an oxygen anion (methoxy). Then, the nucleophilic attack of the adsorbed alcohol to the triglyceride generates a tetrahedral intermediate and as a result, the esters are obtained [24]. A 5% by weight of Na produced an 83 wt% of FAME after 5 h, while 71 wt% of FAME was obtained when the Na loading was 10 wt%. The fact that FAME content did not increase with the alkali metal content can be explained by the lack of the ordered structure of the 10Na/20Ce/SBA-15 catalyst, which gives a poor exposed surface of the active centers and lower total basicity despite its high basic strength, as previously mentioned. Thus, the FAME content is influenced by both the basic strength and the amount of basic sites [30].

However, in these initial reaction conditions, the best catalyst (5Na/20Ce/SBA-15) did not reach the minimum FAME content required by EN 14214. For this reason, different methanol to oil molar ratios were evaluated, aiming to achieve FAME yields that meet the standards (Fig. 8).

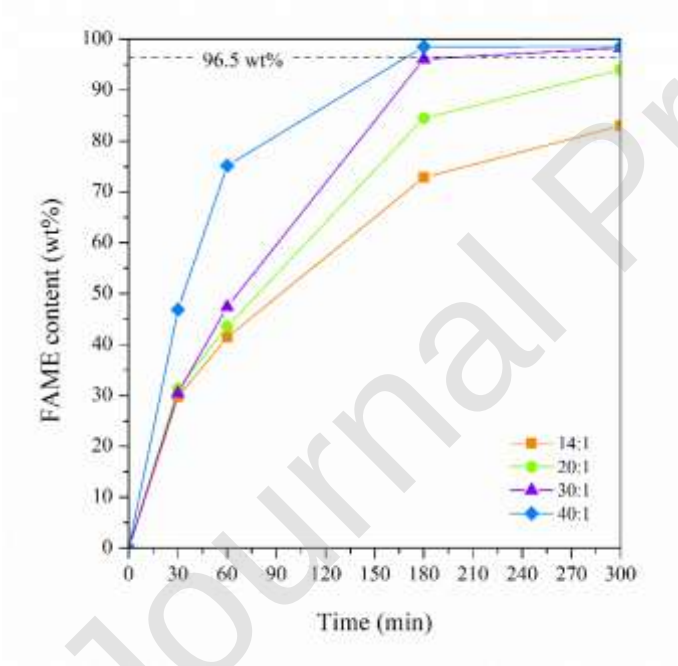

Fig. 8. Effect of methanol to oil molar ratio on FAME content when 5Na/20Ce/SBA-15 is employed as a catalyst. Reaction conditions: 8 wt% of catalyst, 60 °C, magnetic stirring at 600-700 rpm, and 5 h. The dashed line indicates the minimum limit according to European standard EN 14214.

Higher FAME contents were obtained when the methanol content was increased since the reaction rate also increases, reducing the necessary time to reach the required FAME content. 98.5 wt% of biodiesel was reached in 180 min with a 40:1 methanol to oil molar ratio, which shortens the initial reaction time of 5 h. In this way, the use of an excess of methanol served to shift the balance towards the formation of the desired product. Even though increasing the methanol content seems to be a disadvantage, the possibility to recover and reuse it makes this alternative potentially viable.

3.3. Catalyst reusability

The facility of separating and reusing the solid catalyst is an important economic as well as environmental benefit over its homogeneous equivalent [49]. However, one of the main problems that biodiesel production presents when using alkaline solid catalysts is the leaching of the active phase from the surface to the reaction mixture, which shortens the life of the material.

In a previous research, Na/SBA-15 catalysts were studied, which produced FAME contents greater than 96 wt% in the first reaction cycle. However, the activity markedly decreased in the second run, leading to a FAME content near 80 wt% [16]. This was the main reason for introducing a second metal (Ce) as a strategy to stabilize the sodium species and to mitigate leaching.

In consequence, the durability of the 5Na/20Ce/SBA-15 catalyst was investigated. Once the reaction was over, the catalyst was recovered by filtration and washed with acetone to remove any adsorbed compound. Then, the solid was regenerated in an oven for 5 h at 550 °C before the next cycle. The need for a calcination stage before the next run was mentioned by Chen et al., who point out that washing the Na/Zr-SBA-15 catalyst to remove any remaining oil is not completely efficient to recover initial activity [31]. Reactions were carried out under the optimized conditions mentioned above.

As observed in Fig. 9, the catalyst was able to maintain high FAME contents (over 80 wt%) in five reaction cycles, with 91 wt% and 88 wt% of FAME in the second and third reaction cycles. These

results confirm the good stability of the catalyst conferred by Ce addition, together with its better performance compared with that of other Na-modified-SBA-15 catalysts previously studied in the transesterification reaction [16,30,31]. In summary, the catalyst could be used at least for five reaction runs without a significant loss of the activity.

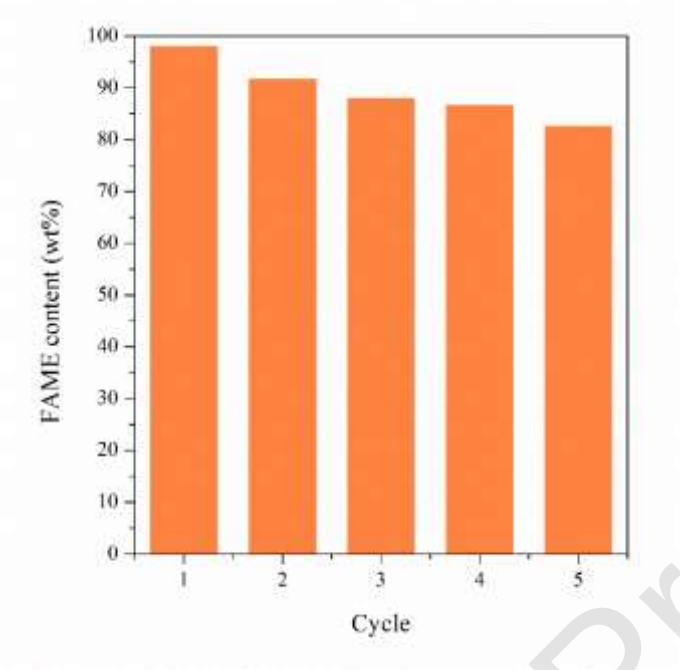

Fig. 9. Reusability of 5Na/20Ce/SBA-15 catalyst. Reaction conditions: 8 wt% of catalyst, 40:1 alcohol to oil molar ratio, 60 °C, magnetic stirring at 600-700 rpm, and 5 h.

Nevertheless, since the obtained FAME contents after cycle 2 are far from the required by the standards, the catalyst concentration was increased to 10 wt%, maintaining the other reaction conditions as mentioned above. In order to preserve the activity, the availability of active centers was increased. Under these conditions, it can be seen in Fig. 10 that, at 180 min, the FAME content exceeds the required by the international standards reaching 99 wt%.

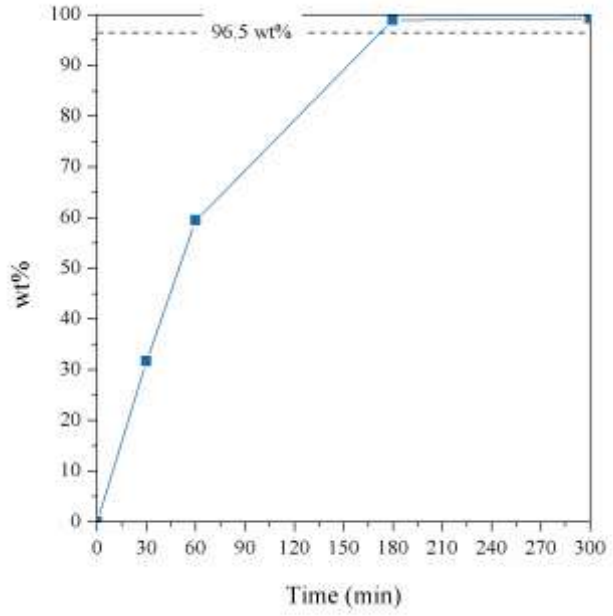

Fig. 10. FAME content vs. reaction time when 5Na/20Ce/SBA-15 is employed as catalyst. Reaction conditions: 10 wt% of catalyst, 40:1 alcohol to oil molar ratio, 60 °C, magnetic stirring at 600-700 rpm, and 5 h. The dashed line indicates the minimum limit according to European standard EN 14214.

Then, as seen in Fig. 11, the reused catalyst was active over four additional cycles in the new reaction conditions. More than 90% by mass of biodiesel was obtained in each of them, being these values within EN 14214 standard until the fourth cycle.

Several studies on solid catalysts showed that the performance of bimetallic catalysts over time is better than that of unimetallic catalysts owing to greater thermal stability and other effects [21,45]. Elías et al. reported the "shielding effect" that a second metal could produce over the first one while coating the catalyst surface with a layer of a metallic oxide, which might prevent leaching of active species during the reaction [29]. In this way, CeO_2 could have a shielding effect on Na species [48]. Furthermore, as reported by Thitsartarn et al., there could also be an interaction between Na and Ce due to some vacancies created by the substitution of Ce ions by Na ions in the ceria phase during calcination. Since the Ce ion on CeO_2 has a valence of 4 and the Na ion has a valence of 1, some vacancies can be created during ion substitution to maintain charge

neutrality on the catalyst surface [6]. This feature can be inferred by the EDS linear chemical composition analysis and when superimposing the EDS mappings (see Fig. S4-b and S5 in *Supplementary Material, respectively*), where sodium (light blue) is found mainly in the vicinity of cerium (fuchsia color) and they are equidistant from each other. These interactions along with the electron transfer between the catalyst components as shown in XPS results may prevent leaching of the metals ions, leading to the high material stability for the transesterification reaction [30]. Contrary to this finding, in the Na/Zr-SBA-15 catalysts reported by Chen et al., Zr could not produce such shielding effect over Na, possibly since it is incorporated into the SBA-15 network by direct synthesis [31].

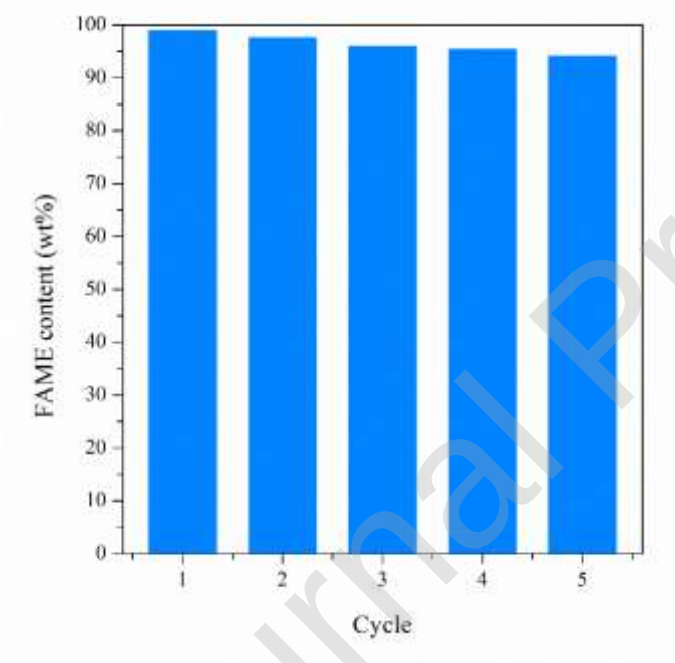

Fig. 11. Reusability of 5Na/20Ce/SBA-15 catalyst. Reaction conditions: 10 wt% of catalyst, 40:1 alcohol to oil molar ratio, 60 °C, magnetic stirring at 600-700 rpm, and 5 h.

Finally, to confirm the heterogeneous catalytic character of the reaction, the hot filtration test was performed [21,49]. After one hour of reaction in the optimized conditions, the solid catalyst was removed by filtration under reduced pressure. Then, the resulting liquid mixture was heated up to 60 °C with magnetic stirring to complete 5 hours while monitoring the FAME content. As Fig.

12 illustrates, after removing the catalyst, biodiesel production ceased, and the percentage by weight of FAME remains relatively constant (~58 wt%). Thus, it can be assumed that homogeneous contribution is not significant to the transesterification activity under optimized reaction conditions.

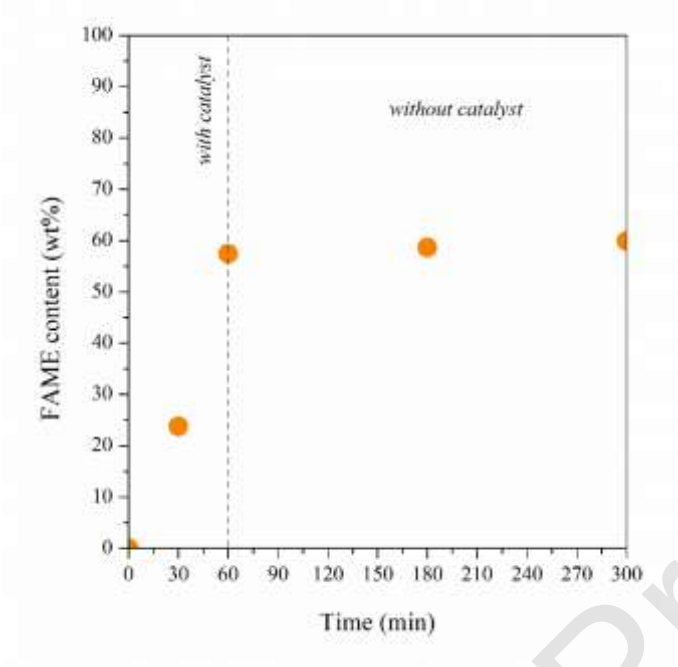

Fig. 12. Hot filtration test for 5Na/20Ce/SBA-15 catalyst. Reaction conditions: 10 wt% of catalyst, 40:1 alcohol to oil molar ratio, 60 °C, magnetic stirring at 600-700 rpm, and 5 h.

3.4. Biodiesel characterization

After optimizing the reaction conditions to achieve the FAME content specified by the European standard EN 14214, employing 5Na/20Ce/SBA-15 as a solid catalyst, key quality parameters of the produced biodiesel were evaluated. This characterization is relevant when the possibilities of corrosion, clogging of the filter, fuel injection problems, and risk in storage and usage exist [24,50,51]. Thus, Table 4 illustrates the main properties of sunflower oil methyl esters obtained. Biodiesel density is important since it influences the injection performance of the biofuel [2,50]. As seen in Table 4, the measured biodiesel density ranges within the established standard values.

Table 4. Physicochemical properties of the obtained biofuel.

Specifications	EN 14214: 2008 limits		Results
	Minimum	Maximum	
FAME content (wt%)	96.5	-	98.9
Density at 15 °C (g/cm^3)	0.86	0.90	0.89
Kinematic viscosity at 40 °C (mm^2/s)	3.5	5	4.9
Acid value ($mg_{KOH}/g_{biodiesel}$)	-	0.5	0.39
Water content (wt%)	-	0.05	0.05

Another parameter that controls the performance of the injectors is the fuel kinematic viscosity. Biodiesel presents greater viscosity than diesel obtained from fossil sources. Nevertheless, unreacted glycerides can increase the viscosity of biofuel. This is why viscosity is also an indicator of the effective conversion of the oil into FAME. Therefore, high values lead to carbon deposition during fuel atomization and reduce combustion efficiency [2,50,52]. The obtained result from the experiments is between the desirable ranges, as seen in Table 4.

The stability of the biofuel is affected by the presence of high levels of free fatty acids (FFA). The FFA concentration is measured through the acid value [2,24,50]. The value resulting from the titration demonstrated that the FAME produced here complies with the standard.

Since excess moisture is detrimental for diesel engines and also affects the biodiesel oxidation stability, it is relevant to measure the water content to determine the storage life of the fuel [2,24,50]. As observed, the obtained biodiesel from the optimized reaction matches the upper limit after methanol recovering.

---

4. Conclusions

Na/Ce/SBA-15 catalysts were successfully prepared by wet impregnation method. Physicochemical characterization served to demonstrate that the highest sodium loading (10%

by mass) produced a marked deterioration of the ordered structure of the material together with a partial blockage of the pores, reducing the exposure of the active sites. However, a loading of 5 wt% of sodium and 20 wt% of cerium resulted effective to achieve a material with good structure, basicity and basic strength necessary to efficiently carry out the transesterification reaction of sunflower oil with absolute methanol. Under optimized reaction conditions (10 wt% of catalyst, 40:1 methanol to oil molar ratio, 60 °C and 700 rpm), a 98.9 wt% biodiesel content was achieved in 3 h. Moreover, this material was successfully reused in five consecutive cycles without further loss of catalytic activity (FAME contents > 90 wt%). Additionally, the biodiesel obtained through this route was characterized, verifying that it meets the requirements of key properties such as density, kinematic viscosity, acid value, and moisture for its commercialization as an alternative fuel, according to EN 14214: 2008 standards. Therefore, the synthesized solid catalyst 5Na/20Ce/SBA-15 may be suitable for large-scale biodiesel production. In addition, its solid-state would allow it to be packed in a fixed bed reactor and thus be used in continuous biodiesel production, which will be subject of future work.

Author contributions

- *Edgar M. Sánchez Faba:* Conceptualization, Formal analysis, Investigation, Methodology, Visualization, Roles/Writing - original draft.
- *Gabriel O. Ferrero:* Conceptualization, Funding acquisition, Methodology, Project administration, Resources, Supervision, Writing - review & editing.
- *Joana M. Dias:* Conceptualization, Methodology, Writing - review & editing.
- *Griselda A. Eimer:* Conceptualization, Funding acquisition, Methodology, Project administration, Resources, Writing - review & editing.

Declaration of interests

☒ The authors declare that they have no known competing financial interests or personal relationships that could have appeared to influence the work reported in this paper.

5. Acknowledgments

The authors are grateful to ANCyT, CONICET-FYPF, and UTN for the financial support through PICT-2016-0472, PIO 13320150100014CO and PID UTN4402. E. M. Sánchez Faba thanks CONICET for the doctoral fellowship and Verónica Brunetti (LAMARX), Fabio Fontanarrosa (SECEGRIN) and Sebastián Eluani for their collaboration. Joana Maia Dias is an integrated member of LEPABE, financially supported by: Base Funding - UIDB/00511/2020 of the Laboratory for Process Engineering, Environment, Biotechnology and Energy – LEPABE - funded by national funds through the FCT/MCTES (PIDDAC).

XPS analysis were performed at Laboratorio de Microscopía Electrónica y Análisis por Rayos X (LAMARX, FaMAF-UNC-CONICET).

References

[1] A.P. Kanakdande, C.N. Khobragade, R.S. Mane, Sustain. Energy Fuels (2020).

[2] C.N. Kowthaman, A.M.S. Varadappan, Int. J. Energy Res. 43 (2019) 3182–3200.

[3] J. Gardy, M. Rehan, A. Hassanpour, X. Lai, A.-S. Nizami, J. Environ. Manage. 249 (2019) 109316.

[4] A.K. Endalew, Y. Kiros, R. Zanzi, Biomass and Bioenergy 35 (2011) 3787–3809.

[5] F. Jamil, L. Al-Haj, A.H. Al-Muhtaseb, M.A. Al-Hinai, M. Baawain, U. Rashid, M.N.M. Ahmad, Rev. Chem. Eng. 34 (2018) 267–297.

[6] W. Thitsartarn, S. Kawi, Green Chem. 13 (2011) 3423.

[7] A.L. de Lima, C.M. Ronconi, C.J.A. Mota, Catal. Sci. Technol. 6 (2016) 2877–2891.

[8] L.C. Meher, C.P. Churamani, M. Arif, Z. Ahmed, S.N. Naik, Renew. Sustain. Energy Rev. 26 (2013) 397–407.

[9] R. Verhé, C. Echim, W. De Greyt, C. Stevens, in: R. Luque, J. Campelo, J. Clark (Eds.), Handb. Biofuels Prod., First ed, Woodhead Publishing Limited, Philadelphia, 2011, pp. 97–133.

[10] E. Santacesaria, G.M. Vicente, M. Di Serio, R. Tesser, Catal. Today 195 (2012) 2–13.

[11] S. Yan, C. Dimaggio, S. Mohan, M. Kim, S.O. Salley, K.Y.S. Ng, Top. Catal. 53 (2010) 721–736.

[12] G.O. Ferrero, E.M. Sánchez Faba, G.A. Eimer, Chem. Eng. J. 348 (2018) 960–965.

[13] D. Kryszak, M. Trejda, N. Benedyczak, M. Ziolek, Catal. Today 325 (2019) 11–17.

[14] J. Dhainaut, J.-P. Dacquin, A.F. Lee, K. Wilson, Green Chem. 12 (2010) 296–303.

[15] H. Wang, Y. Li, F. Yu, Q. Wang, B. Xing, D. Li, R. Li, Chem. Eng. J. 364 (2019) 111–122.

[16] E.M. Sánchez Faba, G.O. Ferrero, J.M. Dias, G.A. Eimer, Catalysts 9 (2019) 690.

[17] J.A. Melero, L.F. Bautista, J. Iglesias, G. Morales, R. Sánchez-Vázquez, Catal. Today 195 (2012) 44–53.

[18] M.C.G. Albuquerque, I. Jiménez-Urbistondo, J. Santamaría-González, J.M. Mérida-Robles, R. Moreno-Tost, E. Rodríguez-Castellón, A. Jiménez-López, D.C.S. Azevedo, C.L. Cavalcante, P. Maireles-Torres, Appl. Catal. A Gen. 334 (2008) 35–43.

[19] I.M. Atadashi, M.K. Aroua, A.R. Abdul Aziz, N.M.N. Sulaiman, J. Ind. Eng. Chem. 19 (2013) 14–26.

[20] A.S. Badday, A.Z. Abdullah, K.T. Lee, M.S. Khayoon, Renew. Sustain. Energy Rev. 16 (2012) 4574–4587.

[21] R. Malhotra, A. Ali, Renew. Energy 119 (2018) 32–44.

[22] E. Leclercq, A. Finiels, C. Moreau, J. Am. Oil Chem. Soc. 78 (2001) 1161–1165.

[23] M. Zabeti, W.M.A. Wan Daud, M.K. Aroua, Fuel Process. Technol. 90 (2009) 770–777.

[24] I. Ambat, V. Srivastava, E. Haapaniemi, M. Sillanpää, Sustain. Energy Fuels 3 (2019) 2464–2474.

[25] T.M. Albayati, A.M. Doyle, J. Nanoparticle Res. 17 (2015) 1–10.

[26] H. Sun, J. Han, Y. Ding, W. Li, J. Duan, P. Chen, H. Lou, X. Zheng, Appl. Catal. A Gen. 390 (2010) 26–34.

[27] W. Thitsartarn, T. Maneerung, S. Kawi, Energy 89 (2015) 946–956.

[28] K. V. Yatish, H.S. Lalithamba, R. Suresh, G.N. Dayananda, Sustain. Energy Fuels 2 (2018) 1299–1304.

[29] V. Elías, E. Sabre, K. Sapag, S. Casuscelli, G. Eimer, Appl. Catal. A Gen. 413–414 (2012) 280–

291.

[30] X. Yu, Z. Wen, H. Li, S.-T. Tu, J. Yan, Fuel 90 (2011) 1868–1874.

[31] W.K. Chen, H.H. Tseng, M.C. Wei, E.C. Su, I.C. Chiu, Int. J. Hydrogen Energy 39 (2014) 19555–19562.

[32] M.R. Anuar, A.Z. Abdullah, Renew. Sustain. Energy Rev. 58 (2016) 208–223.

[33] D. Zhao, J. Feng, Q. Huo, N. Melosh, G.H. Fredrickson, B.F. Chmelka, G.D. Stucky, Science (80-.). 279 (1998) 548–552.

[34] D. Zhao, Q. Huo, J. Feng, B.F. Chmelka, G.D. Stucky, J. Am. Chem. Soc. 120 (1998) 6024–6036.

[35] V. Meynen, P. Cool, E.F. Vansant, Microporous Mesoporous Mater. 125 (2009) 170–223.

[36] E.M. Sánchez Faba, G.O. Ferrero, J.M. Dias, G.A. Eimer, Mol. Catal. 481 (2020) 110171.

[37] N.N. Mahamuni, Y.G. Adewuyi, Energy & Fuels 23 (2009) 3773–3782.

[38] Z.Y. Wu, Q. Jiang, Y.M. Wang, H.J. Wang, L.B. Sun, L.Y. Shi, J.H. Xu, Y. Wang, Y. Chun, J.H. Zhu, Chem. Mater. 18 (2006) 4600–4608.

[39] L.B. Sun, J.H. Kou, Y. Chun, J. Yang, F.N. Gu, Y. Wang, J.H. Zhu, Z.G. Zou, Inorg. Chem. 47 (2008) 4199–4208.

[40] E.-B. Cho, S. Yim, D. Kim, M. Jaroniec, J. Mater. Chem. A 1 (2013) 12595–12605.

[41] N.I. Cuello, V.R. Elías, E. Winkler, G. Pozo-López, M.I. Oliva, G.A. Eimer, J. Magn. Magn. Mater. 407 (2016) 299–307.

[42] N. Pal, E.-B. Cho, A.K. Patra, D. Kim, ChemCatChem 8 (2016) 285–303.

[43] Z. Wen, X. Yu, S.-T. Tu, J. Yan, E. Dahlquist, Appl. Energy 87 (2010) 743–748.

[44] M. Ayoub, A.Z. Abdullah, J. Appl. Sci. 11 (2011) 3510–3514.

[45] R. Malhotra, A. Ali, Renew. Energy 133 (2019) 606–619.

[46] C.D. Wagner, W.M. Riggs, L.E. Davis, J.F. Moulder, Handbook of X-Ray Photoelectron Spectroscopy: A Reference Book of Standard Data for Use in X-Ray Photoelectron Spectroscopy, Perkin-Elmer Corporation, Eden Prairie, 1979.

[47] E. Bêche, P. Charvin, D. Perarnau, S. Abanades, G. Flamant, Surf. Interface Anal. 40 (2008) 264–267.

[48] N. Zhang, H. Xue, R. Hu, RSC Adv. 8 (2018) 32922–32929.

[49] N. Kaur, A. Ali, Appl. Catal. A Gen. 489 (2015) 193–202.

[50] J.M. Dias, M.C.M. Alvim-Ferraz, M.F. Almeida, Fuel 87 (2008) 3572–3578.

[51] G. Knothe, J. Am. Oil Chem. Soc. 83 (2006) 823–833.

[52] C.V.K. de Oliveira, R.F. Santos, J.A.C. Siqueira, R.A. Bariccatti, N.B.G. Lenz, G.S. Cruz, L.K. Tokura, F.F. Klajn, Ind. Crops Prod. 123 (2018) 192–196.